





Theoretical and Applied Mechanics Letters

Volume 13, Issue 1, January 2023, 100418

Letter

Hydrocephalic cerebrospinal fluid flowing rotationally with pulsatile boundaries: A mathematical simulation of the thermodynamical approach

Hemalatha Balasundaram^a, Senthamilselvi Sathyamoorthi^a, Unai Fernandez-Gamiz^b  ,
Samad Noeiaghdam^{c d}, Shyam Sundar Santra^{e f}

[Show more](#) 

 [Outline](#) |  [Share](#)  [Cite](#)

<https://doi.org/10.1016/j.taml.2022.100418> 

[Get rights and content](#) 

Under a Creative Commons [license](#) 

open access

Highlights

- This paper introduces the fluid mechanics of CSF circulation flowing oscillatory inside the cranium system.
- The equation of motion ventricular area inside the porous medium with suitable pulsatile boundary conditions are solved.
- The simulated proposed in this paper is obtained for CSF physio-pathological disease hydrocephalus patients.
- We determine the CSF flow velocity of patients by suitable validity.

Abstract

To study the kinematics of flow rate and ventricular dilatation, an analytical perturbation approach of hydrocephalus has been devised. This research provides a comprehensive investigation of the characteristics of cerebrospinal fluid (CSF) flow and pressure in a hydrocephalic patient. The influence of hydrocephalic CSF, flowing rotationally with realistic dynamical characteristics on pulsatile boundaries of subarachnoid space, was demonstrated using a nonlinear controlling system of CSF. An analytical perturbation method of hydrocephalus has been developed to investigate the biomechanics of fluid flow rate and the ventricular enlargement. In this paper presents a detailed analysis of CSF flow and pressure dynamics in a hydrocephalic patient. It was elaborated with a nonlinear governing model of CSF to show the influence of hydrocephalic CSF, flowing rotationally with realistic dynamical behaviors on pulsatile boundaries of subarachnoid space. In accordance with the suggested model, the elasticity factor changes depending on how much a porous layer, in this case the brain parenchyma, is stretched. It was improved to include the relaxation of internal mechanical stresses for various perturbation orders, modelling the potential plasticity of brain tissue. The initial geometry that was utilised to create the framework of CSF with pathological disease hydrocephalus and indeed the output of simulations using this model were compared to the actual progression of ventricular dimensions and shapes in patients. According to this observation, the non - linear and elastic mechanical phenomena incorporated into the current model are probably true. Further modelling of ventricular dilation at a normal pressure may benefit from the existence of a valid model whose parameters approximate genuine mechanical characteristics of the cerebral cortex.



Keywords

Brain parenchyma; Cerebrospinal fluid; Hydrocephalus; Ventricular elasticity; Intracranial pressure differences

The cerebrospinal fluid (CSF) surrounds the brain, spinal cord, and other components of the central nervous system (CNS). CSF, a fluid that naturally simulates water that flows around the cranium, is secreted by the ventricles of the choroid plexus. It serves as a conduit for the movement of nutrients and neuroendocrine agents that clear waste from the area around the brain. It guards against exogenous injury and traumatic damage to the brain. An aberrant syndrome called hydrocephalus is characterised by the build-up of extra CSF in the ventricular areas. Fluid flow in the ventricular regions is impacted by hydrocephalus, which manifests as an abnormal disturbance in production and circulation. This alteration in the hydrocephalic CSF results in a significant alteration in intracranial pressure, which discharges shunt in the CNS.

The purpose of this paper is to give attention to CSF flowing in an oscillatory motion due to temperature fluctuation with suitable pulsatile boundary conditions. This article is focused on rotationally oriented hydrocephalus featuring inlet pulsatile amplitude modes. To do this, the subarachnoid space fluid movement is predicted using the exacting CSF flow dynamics. In order to assess the thermal approach inside of the brain, Faryami et al. [1] investigated the thermodynamic behaviour of cerebrospinal fluid circulation using a quasi-method. Sincomb [2] created a mathematical equation for the pulsed viscous sequence of CSF in the vertebral column as a first step in allowing such predictive endeavours. The model is based on the assumption that the spine is a linearly elastic compliant duct with time varying segment, and it includes a Darcy force term to model the fluid inertia brought on by the cartilages, which are tiny collagen-reinforced columns that form a web-like structure stretching across the CSF flow rate can be predicted using Fourier-series approximations for realistic anharmonic intracranial pressure (ICP) fluctuations. The projected flow rate at various places throughout the spinal canal roughly corresponds to in person phase-contrast magnetic resonance observations when combined with a representative ICP waveform and a credible canal morphology. The findings show that the suggested model, which only uses a few characteristics, could be used as a base for further studies. The results aim to forecast ICP temporal fluctuations based on observations of spinal-canal geometry and CSF flow rate. In order to permit an elevation in CSF flow rate, the model systematically relates intracranial variations. This flow rate has already been analysed using a harmonic expansion Fourier series. Momjian and Bichsel [3] suggested a better understand the kinematics of ventricular hypertrophy, computational finite element (FE) models of hydrocephalus have been created. Recent linear poro-elastic simulations, although, were unable to replicate the comparatively greater dilation of the lateral ventricle horns. As an alternative, the authors of this work developed a nonlinear poro-plastic finite element model of the brain parenchyma and investigated the impact of adding these possibly more authentic mechanical behaviours on the estimation of the ventricular form. The internal mechanical stress is relieved after each cycle in the current proposal, replicating the likely plastic behaviour of the neural tissue, and the elasticity modulus varies as a function of the distension of the pore spaces. The initial geometry utilised to create the system was taken using Computed tomography of subjects who were developing hydrocephalus, and the simulations' outcomes were evaluated to that same patients' actual changes in ventricle shape and dimension. The magnitude and shape of the ventricular dilatation in actual patients with acute as well as chronically hydrocephalus were successfully predicted by the investigators' model. Hofman and Chen [4] covered a wide range of neurological conditions, including multiple sclerosis, cancer, Alzheimer's disease, and different CSF disorders.

The discovery of more effective treatment alternatives is restricted by the lack of mathematical knowledge of cranial thermodynamics to treat hydrocephalus. Todinova et al. [5] investigated the variations in the thermodynamic characteristics of the unfolding of the two main red blood cell (RBC) proteins—cytoplasmic haemoglobin (Hb) and membrane Band 3 (B3) protein—can distinguish neurodegenerative disorders from the healthy normal condition. The greater thermal stability of the Hb and B3 proteins as RBCs age is a characteristic of neurodegenerative disorders (NDDs), and calorimetric enthalpy can distinguish Parkinson's disease (PD) from amyotrophic lateral sclerosis (ALS) and Alzheimer's disease (AD). Our findings offer insights into the thermodynamic behaviour of RBCs in

two intricately intertwined processes—neurodegenerative dysfunctions and aging—and imply that the calculated thermodynamic metrics are signatures of the disrupted Hb and B3 structure formation and modified RBC ageing in the investigated NDDs. Ursino [6] Appropriate values for the model's parameters were determined by considering contemporary anatomical data and physiological factors. In their study, the form and genesis of the intracranial pressure pulse wave are simulated using a mathematical model. Particularly, the model's prediction of the relationship between mean intracranial pressure and intracranial pressure pulse amplitude exhibits outstanding concordance with previous experimental observations. The cerebrovascular compliance-related pulsing variations in cerebral blood volume that take place within a rigid area are what cause the ICP pulse wave, according to the model (i.e., the craniospinal compartment). The brain pressure-volume connection is mostly reflected by the intracranial pressure pulse amplitude for low and average intracranial pressure levels. But in cases of severe intracranial hemorrhage, there is a sudden rise in cerebrovascular resistance, which is reflected in the pulse wave of intracranial pressure.

The lateral ventricles were expected to experience the maximum pressure amplitude. It was discovered that the pressure wave frequency as in vertebral column nearly matched the values previously reported in the literature. To create a fundamental knowledge of the connections between vascular pulsations, CSF flow, and CSF pressure waves in the CNS, the numerical method presented by Lininger et al. [7] to investigate the three-dimensional CSF flow field within a healthy subject's CNS was measured using cine-phase-contrast-MRI (magnetic resonance imaging). A three-dimensional dynamic interaction model of the CSF flow inside the CNS was subsequently created using methods for image restoration and grid creation. Through using finite-element approach, the equations governing for fluid and solid motion have been computed in ADINA-FSI 8.6, and also the CSF regions were then discretized. The empirical methods and model estimates of CSF velocity magnitude and stroke volume were found to be in very good agreement. CSF pressure gradients and amplitudes were computed in all regions of the CNS. The pressure gradients and amplitudes estimated closely resemble those measured in clinical settings. Struan et al [8] experimented data revealed an asymmetric flow pattern in the aneurysm. The model of asymmetric pulsatile flow model is validated by computational method to simulate the thrombin transport, by using an inlet boundary of data-derived flow function by using both steady and transient state. Gholampour et al. [9] modelled computational method for CSF mean pressure amplitude and pressure.

Sharp et al. [10] described a dynamical model by Taylor's dispersion in the superior subarachnoid space and “glymphatic system” areas that may clinically controlled to improve fluid transport. Herbowski and Gurgul [11] illustrated circulation of CSF with thermodynamics behaviour to show the temperature variation between superior subarachnoid space in the intracranial and intracanal compartments. It might cause natural circulation of CSF with a constant temperature. He developed a model of cerebrospinal fluid flow with the Brownian movements due to gravitational force creates molecular motion. The cerebrospinal fluid circulation in the spinal canal is like a corkscrew motion due to its structure. Greco et al. [12] validated analytical determination CSF disorders (acute disseminated encephalomyelitis; multiple sclerosis), chronic neurodegenerative diseases like Alzheimer disease;

Parkinson disease and some neurological diseases. The method of chromatographic results sensitive behaviour of CSF flow.

The study suspects the clinical report on neurological disease of CSF H₂S concentrations and shows the new perspectives on the clinical relevance of H₂S and its application. Donnelly and Czosnyka [13] proved the likelihood of unstable behaviour seems to be increased in the absence of large-volume blood flow to lower and maintain the brain temperature. The temperature of the brain tissue is often warmer than that of outflowing venous blood, which is typically warmer than that of inflowing arterial blood. Thus, brain blood flow might be thought of as a brain warmer. In addition to a brief overview of the fundamental information on temperature, cerebral blood flow and volume, intracranial pressure, and compartmental compliances of the brain, a multifunctional controls and procedures are addressed. Linninger et al. [7] suggests a meticulous computational model for precisely forecasting the behaviour of therapeutic drugs injected into the brain. Data from in-vivo diffusion tensor magnetic resonance imaging are used to explain the geometrical and physical characteristics of anisotropic and varied brain tissue that affect medication delivery. From particular aspect diagnostic scans, a precise reconstruction of the three-dimensional brain anatomy is made. Diffusion tensor imaging is used to quantify tissue variability and distortion. To anticipate the outcome of a high-molecular weight nutritive factor pumped into the cerebrum, fundamental diffusion phenomena are exploited. There hasn't been enough study done in the open literature on computer prediction of drug distribution in humans accounting for diverse and asymmetrical brain tissue features. Raptis and Singh [14] study the effect of rotation on the free convection flow of an electrically conducting and viscous incompressible fluid past a uniformly accelerated vertical plate in a magnetic field. The temperature of the plate differs from the temperature of the fluid, causing the free convection flow in the boundary layer. A mathematical model of CSF flow factors with a thermal physical approach was constructed by Hemalatha and Sathiamoorthy [15] in two layers of the cranium, including the brain parenchyma and hydrocephalus. They also demonstrated specific CSF velocity outcomes as a function of increasing parameters like the Darcy number, the resistance parameter, etc. H Hemalatha and Senthamil Selvi [16] and Balasundaram et al. [17] analyzed a hydrodynamical model for congenital hydrocephalus in laminar flow that has been manipulated using perturbation method to validate the clinical studies.

The recent study of CSF by Gholampour et al. [18], [19], [20] examined the changes in the various parameters and clinical features of the disease before the treatment process of communicating and non-communicating hydrocephalus. 13 healthy participants, 11 non-communicating hydrocephalus (NCH) sufferers in the pre-treatment stage, and 3 patients in the five post-treatment stages were all simulated using 3D dynamic interaction modelling. While the flow remains homogeneous, NCH increases the vortex and pulsatility of the CSF flow. Maximum CSF pressure has reduced in direct proportion to the degree of medical symptom improvement, has recovered more quickly than other measures to the pressure range seen in normal people, and has done so at the same time that patients' clinical symptoms have vanished. After shunting and recovery, patients have experienced a new healthy state in new hydrodynamic circumstances. An improved non-invasive technique was used to estimate patients' cerebral perfusion compliance following shunting compared to earlier experimental techniques. Gaining deeper understanding of the pathophysiology of NCH patients can be aided by

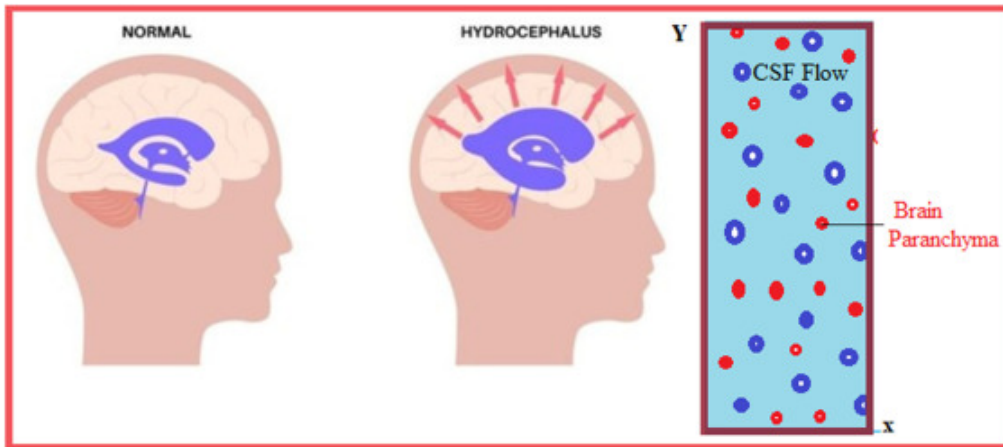
changes in hydrodynamic parameters as well as clinical reports from patients. Recent effects on mucus fluid with the explosion of pandemic Covid-19 was examined by Thiagarajan et al [21,22], Padmavathi et al. [23] and magnetohydrodynamics in porous media with diverse effects was demonstrated by Vijayalakshmi et al [24]. Gholampour and Fatourae [25] proposed eight healthy individuals and 11 hydrocephalus patients had their cine phase-contrast MRI data utilised to create 3D cranial geometric representations, which were then employed in computer simulations under three different inlet/outlet boundary conditions (BCs). The ventricular system volume and the maximal CSF pressure were more precise and efficient compared to other indicators in assessing the sufferers' condition. The computational patient models were 18.5% more sensitive to CSF volume changes in the ventricular system under BC when the CSF pressure was constant. It was proposed to employ pulsatile CSF flow rate diagrams for the inflow and outflow BCs to assess the patients with hydrocephalus' intracerebral compliance. The findings recommended employing the fully coupled fluid-structure interaction (FSI) approach and the computational fluid dynamic (CFD) method, accordingly, for the CSF simulation process in subjects with exterior and interior hydrocephalus.

In our earlier studies, we extensively examined the CSF flow with elastic boundary travelling in a laminar flow confined with porous layer for sufferers with hydrocephalus. Our aim is to predict the flow velocity and the ICP differences of CSF syndrome like hydrocephalus. As a result of the interplay between the thermal solid model and the motion of the CSF caused by the hydrocephalus flowing inside the vertebral column, we have included an elasticated effect in the current work. In other words, utilising diffused finite volume, finite element, and analytical approaches, we have created a new approach to account for CSF flow behavior considering effects of boundary thermal effects. This paper is the extension of previous paper [16] expels the pulsatile flow with thermodynamical changes flowing rotationally. we developed a model of poro-elastic deformation of brain parenchyma due to hydrocephalus disorder. In this present work, we include the pressure variation an oscillatory flow due to hydrocephalus with thermodynamical approach. In this paper, we investigated our flow methodology which includes governing equations with inlet pulsatile boundary conditions. The significance of analytical methods was generated with experimental studies of neurologists.

CSF is a Newtonian incompressible fluid that has the density and dynamic viscosity of water, $998.2 \text{ kg}\cdot\text{m}^{-3}$ and $1.003 \times 10^{-3} \text{ kg}\cdot\text{m}^{-1}\cdot\text{s}^{-1}$ respectively. We employ these values as an amplitude as an inlet CSF fluid of pulsatile flow rate utilising the perturbation approach analytically [9]. We take measurements the elasticity of brain tissue is unknown experimentally, we assess the elasticity of normal brain tissue, which ranges from 10 to 100 KPa as suggested by Ref. [3]. Every human person secretes between 400 and 600 ml of CSF each day. The situation changes, nevertheless, depending on the age group. Additionally, arachnoid villi that travel through the central nervous system for cardiac circulation reabsorb CSF for normal persons as blood [6]. The brain's true shape will be maintained throughout this procedure. The condition known as hydrocephalus is caused by an excessive amount of CSF secretion that is abnormal [9].

Since the human brain is much related to rigorous fluid mechanics, its techniques are used to generate the geometry of CSF flow. Considering a hydrodynamic oscillatory flow of an incompressible, unsteady viscous fluid moving in pulsatile along the boundaries vertically in a finite medium embedded with

brain parenchyma. Also, we describe the coordinate system in a horizontal and vertical directions on x -axis and y -axis respectively. Let Ω_h represent the control volume of CSF flow and $\partial\Omega_h$ represent its boundary. Meanwhile, fluid particle rotating in a uniform velocity Ω with respect to y -axis. Consequently, u and v resembles the velocity of fluid flow in x and y respectively. Considering the fluid initially, at rest portion with uniform temperature and all the physical quantities depend only on y and t . Then the fluid particle starts moving at a time t and it is maintained uniformly throughout the fluid moment is expressed in Fig. 1. we neglect gravitational forces in the fluid flow for our convenience.



[Download : Download high-res image \(253KB\)](#)

[Download : Download full-size image](#)

Fig: 1. Flow geometry

The subarachnoid space experiences high-pressure fluid flow as a result of hydrocephalus. Due to the flexibility of the ventricles brought on by the resistance of excessive fluid secretion, we attempted to demonstrate the flow amplitude of the hydrocephalus patients. Since the human brain and exact fluid mechanics are closely coupled, these techniques are employed to create the geometry of CSF flow. The experimental strategy to anticipate neurologists' conceptual framework may be justified by the analytical procedure simulated. The governing equations for a homogeneous porous media and an unstable incompressible viscous fluid in natural convection are given by

$$\frac{\partial u}{\partial x} + \frac{\partial w}{\partial y} = 0, \quad (1)$$

$$\frac{\partial u}{\partial t} + Gw_0 \frac{\partial u}{\partial y} + 2\Omega' w = -\frac{1}{\rho} \frac{\partial p}{\partial x} + \nu \left(\frac{\partial^2 u}{\partial y^2} \right) - \frac{\nu}{K} u + \frac{RN}{\rho} u, \quad (2)$$

$$\frac{\partial w}{\partial t} + Gw_0 \frac{\partial w}{\partial y} - 2\Omega' u = -\frac{1}{\rho} \frac{\partial p}{\partial y} + \nu \left(\frac{\partial^2 w}{\partial y^2} \right) - \frac{\nu}{K} w + \frac{RN}{\rho} w \quad (3)$$

$$\left(\frac{\partial T}{\partial t} + w_0 \frac{\partial T}{\partial y} \right) = \frac{k}{\rho C_p} \left(\frac{\partial^2 T}{\partial y^2} \right) + \frac{J}{\rho C_p} (T - T_c), \quad (4)$$

$$u = \omega \left(\cos \omega t + \frac{1}{2} \sin \omega t \right), w = 0, T = T_0 \text{ at } y = 0 \text{ and } t \leq 0,$$

$$u = u_0 \omega (1 + \cos \lambda t) \cos n \omega t, w = 0, T = T_c \text{ at } y = 1, t > 0, \quad (5)$$

$$\frac{\partial p}{\partial x} = \omega e^{-\omega t}. \quad (6)$$

We use pulsatile inlet boundary condition of Ref. [7] to specify the flow of CSF in the cranium layer. Non-dimensional quantities relevant to the problem and neglecting the dash symbol for our convenience

$$y' = \frac{y}{l}, \quad t' = \frac{tw_0}{l}, \quad w' = \frac{wl}{w_0}, \quad u' = \frac{u}{u_0}, \quad \omega' = \frac{\omega l^2}{\nu},$$

$$\theta' = \frac{T-T_c}{T_0-T_c}, \quad Re = \frac{w_0 l}{\nu}, \quad G_{pm} = \frac{RNl^2}{\mu}, \quad Pr = \frac{\rho c_p l w_0}{k}, \quad J = \frac{kl}{\rho c_p w_0}, \quad \Omega' = \frac{\Omega l^2}{\nu}.$$

u and w refer the velocity of fluid in x and y direction respectively. w_0 is represented as characteristic velocity. Fluid density is referred as ρ , θ refers as temperature of fluid. Da and Ω expressed as Darcy number and angular velocity, G_{pv} and Pr referred as particle mass parameter and Prandtl number, heat conduction parameter is represented as J , T_c referred as boundary temperature of CSF. T_0 refers free steam temperature of CSF. ω represents Womersley number of CSF fluid.

The following were the governing Eqs.(1) to (5) in dimensionless form

$$Re \left(\frac{\partial u}{\partial t} + G \frac{\partial u}{\partial y} \right) + 2\Omega w = -\alpha^2 e^{\zeta t} + \frac{\partial^2 u}{\partial y^2} - \frac{1}{\sigma^2} u + G_{pv} u \quad (7)$$

$$Re \left(\frac{\partial w}{\partial t} + G \frac{\partial w}{\partial y} \right) - 2\Omega u = -\alpha^2 e^{\zeta t} + \frac{\partial^2 w}{\partial y^2} - \frac{1}{\sigma^2} w + G_{pv} w \quad (8)$$

$$\frac{\partial \theta}{\partial t} + \frac{\partial \theta}{\partial y} = \frac{1}{Pr} \frac{\partial^2 \theta}{\partial y^2} + J\theta, \quad (9)$$

corresponding initial and boundary conditions are,

$$u = \alpha^2 \left(\cos \zeta t + \frac{1}{2} \sin \zeta t \right), \quad w = 0, \quad \theta = 1 \quad \text{at } y = 0$$

$$u = \alpha^2 \cos n\zeta t, \quad w = 0, \quad \theta = 0 \quad \text{at } y = 1, \quad n \text{ is an integer.} \quad (10)$$

u and w are functions of x and y , as we considered the fluid flows rotationally. To solve the above momentum equation, we introducing the complex velocity, $F = u + iw$.

The momentum equation in an explicit form of complex function which changes the equation of motion as follows

$$Re \left(\frac{\partial F}{\partial t} + G \frac{\partial F}{\partial y} \right) + 2\Omega IF = -2I\alpha^2 e^{\zeta t} + \frac{\partial^2 F}{\partial y^2} - \frac{1}{\sigma^2} F + G_{pv} F. \quad (11)$$

We assume a suitable boundary condition $F = \alpha^2 \left(\cos \zeta t + \frac{1}{2} \sin \zeta t \right)$, $y = 0$, $t \leq 0$.

$$F = \alpha^2 \cos n\zeta t, \quad y = 1, \quad t > 1. \quad (12)$$

With the aid of a model problem, we employ analytical techniques to comprehend the biologically advantageous nature of the brain's mechanisms and their physical impacts. The effectiveness of the numerical method might also benefit from the analytical method. As a result, we reduce those equations to an ordinary differential equation and solve the equation analytically. We solve the above

governing equation using perturbation technique as the method is quite error less in nature, assuming the trail solution for velocity, diffusivity and heat transfer as

$$F(y, t) = F_0(y) + \frac{\epsilon}{2} e^{i\lambda t} F_1(y) + \frac{\epsilon}{2} e^{-i\lambda t} F_2(y), \quad (13)$$

$$\theta(y, t) = \theta_0(y) + \frac{\epsilon}{2} e^{i\lambda t} \theta_1(y) + \frac{\epsilon}{2} e^{-i\lambda t} \theta_2(y). \quad (14)$$

λ refers to oscillation frequency and ϵ being an arbitrary constant parameter defined in such a way that $\epsilon \ll 1$. Let us consider u_0, u_1, u_2 refers zero order, first order and second orders of momentum equation respectively. $\theta_0, \theta_1, \theta_2$ refers zero order, first order and second orders of energy equation respectively. I and i represents the complex variable of the above equations of F and u respectively

The above equation is solved by analytical way of perturbation method that results as

$$F_0 = \alpha^2 e^{m_1 y} - A_2 (e^{m_1 y} - e^{m_2 y}) + \frac{2\alpha^2}{a} (e^{m_1 y} - 1), \quad (15)$$

$$F_1 = \alpha^2 \left(\cos \zeta t + \frac{1}{2} \sin \zeta t \right) e^{m_3 y} - \frac{(e^{m_3 y} - e^{m_4 y})}{(e^{m_3} - e^{m_4})} \left[\alpha^2 \left(\cos \zeta t + \frac{1}{2} \sin \zeta t \right) e^{m_3} - \alpha^2 \cos \zeta t + \frac{2\alpha^2 e^{\zeta t}}{b} (e^{m_3} - 1) \right] + \frac{2\alpha^2}{a} (e^{m_1 y} - 1), \quad (16)$$

$$F_2 = \alpha^2 \left(\cos \zeta t + \frac{1}{2} \sin \zeta t \right) e^{m_5 y} - \frac{(e^{m_5 y} - e^{m_6 y})}{(e^{m_5} - e^{m_6})} \left[\alpha^2 \left(\cos \zeta t + \frac{1}{2} \sin \zeta t \right) e^{m_5} - \alpha^2 \cos \zeta t + \frac{2\alpha^2 e^{\zeta t}}{b} (e^{m_5} - 1) \right] + \frac{2\alpha^2}{a} (e^{m_1 y} - 1), \quad (17)$$

$$\theta_0 = A_7 e^{m_7 y} + A_8 e^{m_8 y}, \quad (18)$$

$$\theta_1 = A_9 e^{m_9 y} + A_{10} e^{m_{10} y}, \quad (19)$$

$$\theta_2 = A_{11} e^{m_{11} y} + A_{12} e^{m_{12} y}. \quad (20)$$

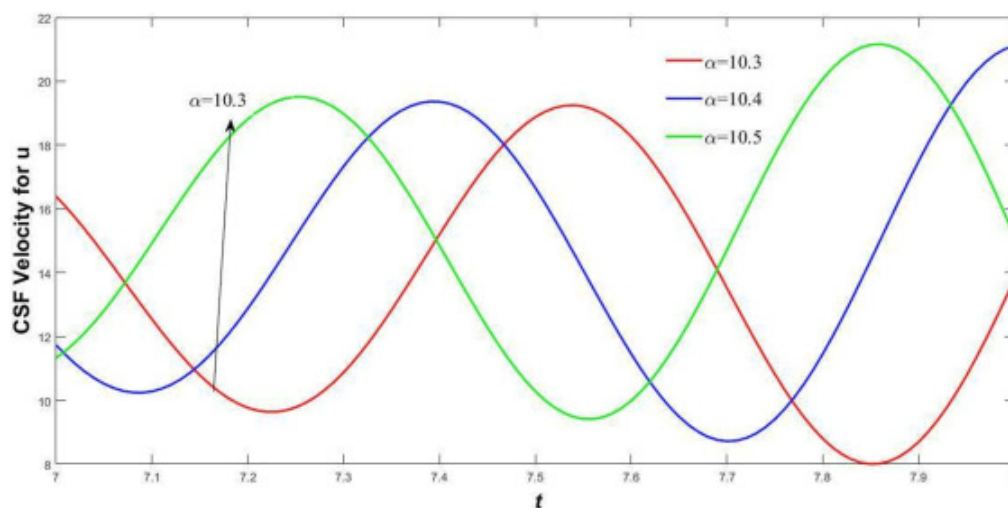
In order to explore the various physical parameters such as dynamic viscosity μ , density, kinematic viscosity, Particle mass parameter, Elasticity, Prandtl number for heat transfer, Reynolds number, Darcy number, and Heat conduction parameter, these have been determined analytically and the results were plotted by using MATLAB. The intracranial pressure of normal subject human being was found to be 500 Pa and 3000 Pa for hydrocephalus patients [7]. Dimension of lateral ventricle for hydrocephalus exceeds 27.2 times more than normal CSF. Also, third and fourth ventricle elastance increases nearly 60% and 40% more than the normal CSF flow. Hence there is a significant difference in ventricular enlargement for hydrocephalus.

Despite of physical brain geometry, the principle of fluid mechanics needs some physical parameters with respect to the CSF flow nature. The parametric values include viscosity (μ), porosity (φ),

permeability of tissue (k), density (ρ). Also, Reynolds number (Re), pressure (P), Womersley number (α) for normal subject and Hydrocephalus patient are listed in [Table 2](#).

The following graphs we summarized the system of Governing Equations the region, with the boundary conditions are solved analytically. To understand the behaviour of the oscillating flow characteristics, velocity (F), temperature (θ) are calculated by varying the emerging flow parameters like Reynolds number, Prandtl number, Darcy number, Elastic parameter, particle mass parameter, heat conduction parameter and so on.

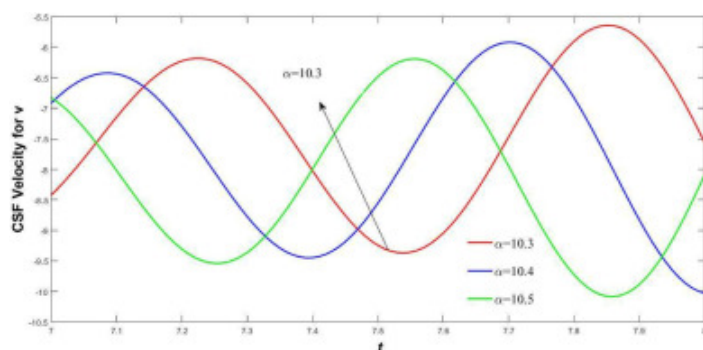
At the earlier systole of cardiac cycle, the velocity in real ([Fig. 2](#)) and imaginary part ([Fig. 3](#)) of CSF flow reaches peak level when there is change in flow frequency. When the frequency increases with the time period the flow rate of hydrocephalus decreases with respect to time taken. Hence increase on Womersley number for pulsatile flow velocity acquires the maximum flow volumetric flow rate.



[Download : Download high-res image \(344KB\)](#)

[Download : Download full-size image](#)

Fig. 2. Womersley number variation in real part of CSF velocity with change in time

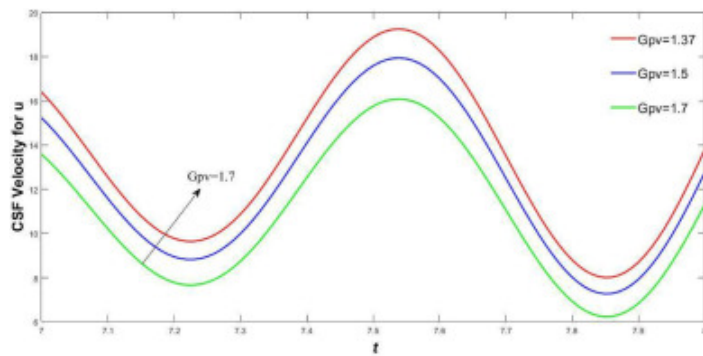


[Download : Download high-res image \(210KB\)](#)

[Download : Download full-size image](#)

Fig. 3. Womersley number variation in imaginary part of CSF velocity with change in time.

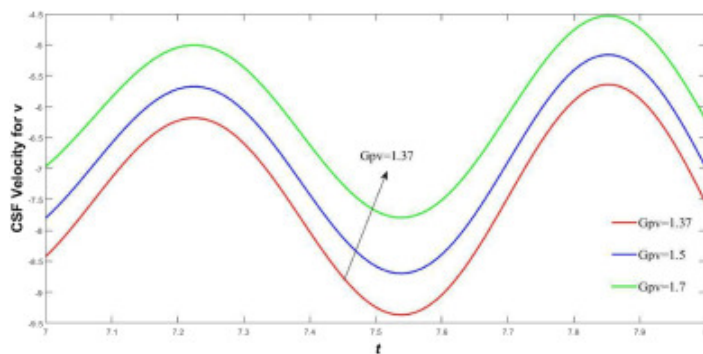
In Fig. 4, Fig. 5, the Resistance parameter increases the in velocity of hydrocephalus attains the maximum level. Moreover, in Fig. 6, Fig. 7 the ventricular elasticity deforms as the fluid level accumulates the SAS. Darcy number plays a vital role in the hydrocephalus fluid flow movements. The porosity of brain parenchyma is estimates as 0.2 [7], Darcy number is calculated with the permeability of the tissue, through which the fluid flow with high pressure. Hence the fluid amplitude increases as the Darcy number parameter escalates proves the high-pressure CSF fluid flow shown in Fig. 8, Fig. 9.



Download : [Download high-res image \(209KB\)](#)

Download : [Download full-size image](#)

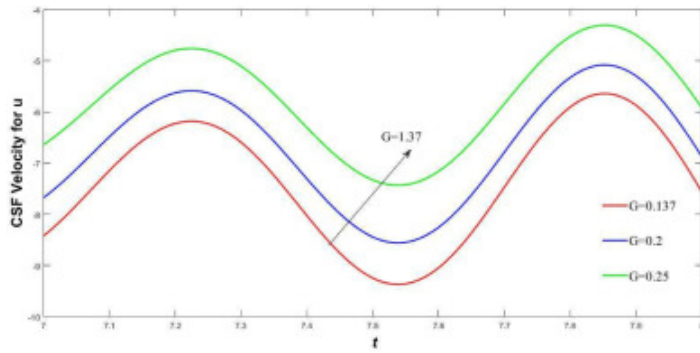
Fig. 4. Gpv variation in real part of CSF velocity with change in time



Download : [Download high-res image \(203KB\)](#)

Download : [Download full-size image](#)

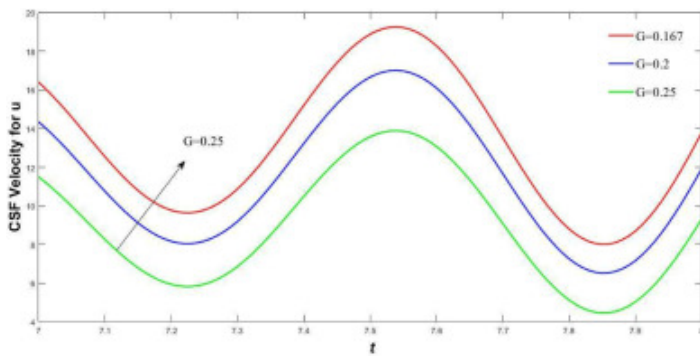
Fig. 5. Gpv variation in imaginary part of CSF velocity with change in time



[Download : Download high-res image \(191KB\)](#)

[Download : Download full-size image](#)

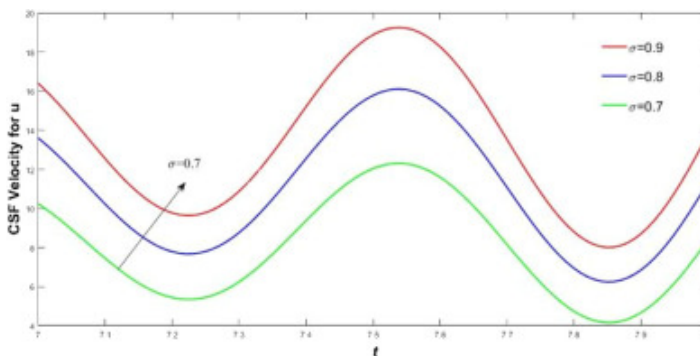
Fig. 6. Elasticity parameter in real part of CSF velocity with change in time



[Download : Download high-res image \(203KB\)](#)

[Download : Download full-size image](#)

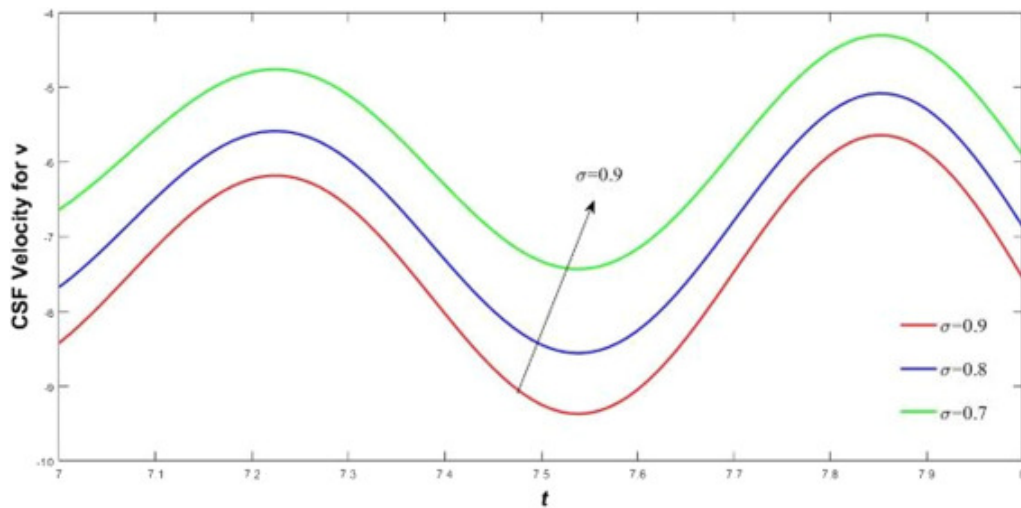
Fig. 7. Elasticity variation in imaginary part of CSF velocity with change in time



[Download : Download high-res image \(157KB\)](#)

[Download : Download full-size image](#)

Fig. 8. σ variation in real part of CSF velocity with change in time

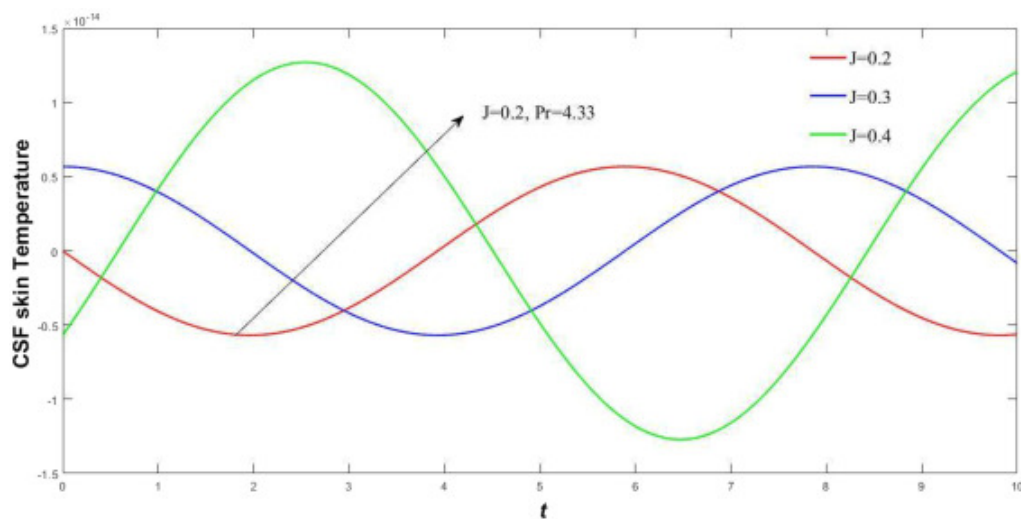


[Download : Download high-res image \(238KB\)](#)

[Download : Download full-size image](#)

Fig. 9. σ variation in imaginary part of CSF velocity with change in time limit.

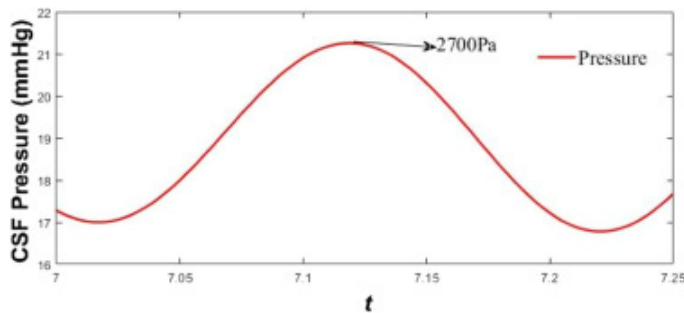
Figure 10 resembles the skin temperature of subarachnoid space (SAS) where fluid accumulates excessively, when the heat conduction parameter increases with the Prandtl number of water (as CSF is a Watery fluid) the heat conductivity accelerates with time variation. Hence there is a temperature fluctuation in case of Hydrocephalus patients. As it deforms the condition of patient will be abnormal which leads to increase in pressure Fig. 11. The pressure of hydrocephalus is more than 2700 Pa whereas for normal subjects is not more than 500 Pa [9]. We validate the increase in pressure graphically.



[Download : Download high-res image \(273KB\)](#)

[Download : Download full-size image](#)

Fig. 10. Heat conduction variation in SAS boundary temperature with change in time



[Download : Download high-res image \(81KB\)](#)

[Download : Download full-size image](#)

Fig. 11. Pressure variation in CSF velocity with change in time

In brain hydrocephalus, pressure difference varies significantly due to the influences of high CSF pulsatile velocity. This results in increase in ventricular enlargement of cranial system is clearly demonstrated in [Table 1](#). There agrees with the lesser compliance of ventricular when there is an increase in pressure. CSF circulation and production will affect the entire function of affected patients that leads to a brain damage.

Table 1. Dimension of Normal and Hydrocephalus subjects [7]

Ventricles	Normal subject	Hydrocephalus patient
Lateral	9.2 cm ³	250.2 cm ³
Third	2.48 cm ³	11.3 cm ³
Fourth	3.31 cm ³	4.57 cm ³

Table 2. To compute the validity of rotational effects in pulsatile flow we use the following parametric values

S. No	Parameters	Value	
		normal	Hydrocephalus
1	Permeability of tissue	$0.7 \times 10^{-15} \text{ m}^2$ [7]	$0.67 \times 10^{-16} \text{ m}^2$ [7]
2	Porosity	0.3 [7]	0.25 [7]
3	Pressure gradient	500 Pa [9]	2700 Pa [9]
4	Elasticity	350 Pa	
5	Reynolds Number	300 [19]	468.3 [19]
6	Womersley Number	3.2 [19]	≥ 8.9 [19]
7	Void space	0.2 [9]	-

S. No	Parameters	Value	
		normal	Hydrocephalus
8	Resistance parameter	1.367 [3]	-

This paper introduces the fluid mechanics of CSF circulation flowing oscillatory inside the cranium system. The equation of motion ventricular area inside the porous medium with suitable pulsatile boundary conditions were solved. The simulated proposed in this paper is obtained for CSF physio-pathological disease hydrocephalus patients. We determined the CSF flow velocity of patients by suitable validity.

The relevant parameters like Womersley number, elasticity, particle mass parameter, Darcy number predict the flow level in cardiac cycle. Heat conduction parameter graph shows the temperature variation which shows an abnormal function of brain behaviour. This study, in an idealized model of the hydrocephalus appropriate to neurological studies, has validated few interesting features of fluid behaviour in thermal transport the following were the conclusions as identified from the present investigation.

1. The momentum of fluid flow enhances for increasing Darcy number, resistance parameter, Womersley number and Reynolds number.
2. Increase in deformation (elasticity) with means of dimensional change results in increase in cerebrospinal fluid velocity.
3. There is a temperature fall influencing a significant difference in the enhancement of heat conduction parameter and Prandtl number. Also, An excess pressure expels critical behaviour of cerebrospinal fluid flow which results in speedy medication.

This paper might support the researchers who deal experimentally with the pathophysiological disorders like hydrocephalus, Parkinson disease, Meninges diseases etc. Further, this paper can be extended for pulsatile behaviour during inlet and outlet velocity with solute diffusivity of viscoelasticity due to high pressure change.

This paper might support the researchers who deal experimentally with the pathophysiological disorders like hydrocephalus, Parkinson disease, Meninges diseases etc. Further, this paper can be extended for pulsatile behaviour during inlet and outlet velocity with solute diffusivity of viscoelasticity due to high pressure change.

Declaration of competing interest


The authors declare that they have no known competing financial interests or personal relationships that could have appeared to influence the work reported in this paper.

Acknowledgements

The work of U.F.-G. was supported by the government of the Basque Country for the [ELKARTEK21/10 KK-2021/00014](#) and [ELKARTEK22/85](#) research programs, respectively.

[Recommended articles](#)

References

- [1] A. Faryami, A. Menkara, D. Viar, *et al.*
Testing and validation of reciprocating positive displacement pump for benchtop pulsating flow model of cerebrospinal fluid production and other physiologic systems
PLoS One, 17 (2022), Article e0262372
[CrossRef ↗](#) [View in Scopus ↗](#) [Google Scholar ↗](#)
- [2] S. Sincomb, W. Coenen, C. Gutiérrez-Montes, *et al.*
A one-dimensional model for the pulsating flow of cerebrospinal fluid in the spinal canal
J. Fluid Mech., 939 (2022), p. A26
[View in Scopus ↗](#) [Google Scholar ↗](#)
- [3] S. Momjian, D. Bichsel Shahan
Nonlinear poroplastic model of ventricular dilation in hydrocephalus
J. Neurosurg., 109 (2008), pp. 100-107
[View in Scopus ↗](#) [Google Scholar ↗](#)
- [4] F.M. Hofman, T.C. Chen
Choroid plexus: structure and function
Choroid Plexus Cerebrospinal Fluid (2016), pp. 29-40
 [View PDF](#) [View article](#) [View in Scopus ↗](#) [Google Scholar ↗](#)
- [5] T. Svetla, S. Krumova, D. Bogdanova, *et al.*
Red blood cells' thermodynamic behavior in neurodegenerative pathologies and aging
Biomolecules, 11 (2021), p. 1500
[Google Scholar ↗](#)
- [6] M. Ursino
A mathematical study of human intracranial hydrodynamics part 1—the cerebrospinal fluid pulse pressure
Ann. Biomed. Eng., 16 (1988), pp. 379-401
[View in Scopus ↗](#) [Google Scholar ↗](#)
- [7] A. Linninger, M. Xenos, D.C. Zhu, *et al.*
Cerebrospinal fluid flow in the normal and hydrocephalic human brain

IEEE Trans. Biomed. Eng., 54 (2007), pp. 291-302

[View in Scopus ↗](#) [Google Scholar ↗](#)

- [8] S. Hume, J.I. Tshimanga, P. Geoghegan, *et al.*
Effect of pulsatility on the transport of thrombin in an idealized cerebral aneurysm geometry

Symmetry, 14 (2022), p. 133

[CrossRef ↗](#) [View in Scopus ↗](#) [Google Scholar ↗](#)

- [9] S. Gholampour, N. Fatourae, A.S. Seddighi, *et al.*
Numerical simulation of cerebrospinal fluid hydrodynamics in the healing process of hydrocephalus patients

J. Appl. Mech. Tech. Phys., 58 (2017), pp. 386-391

[CrossRef ↗](#) [View in Scopus ↗](#) [Google Scholar ↗](#)

- [10] M.K. Sharp, R.O. Carare, B.A. Martin
Dispersion in porous media in oscillatory flow between flat plates: Applications to intrathecal, periarterial and paraarterial solute transport in the central nervous system

Fluids Barriers CNS, 16 (2019), pp. 1-17

[View in Scopus ↗](#) [Google Scholar ↗](#)

- [11] L. Herbowski, H. Gurgul
thermodynamic approach to cerebrospinal fluid circulation

J. Neurol. Res., 1 (2011), pp. 215-218

[Google Scholar ↗](#)

- [12] V. Greco, C. Neri, D. Pieragostino, *et al.*
Investigating different forms of hydrogen sulfide in cerebrospinal fluid of various neurological disorders

Metabolites, 11 (2021), p. 152

[CrossRef ↗](#) [View in Scopus ↗](#) [Google Scholar ↗](#)

- [13] J. Donnelly, M. Czosnyka
The thermodynamic brain



Crit. Care, 18 (2014), pp. 1-2

[Google Scholar ↗](#)

- [14] A. Raptist, A.K. Singh
Rotation effects on MHD free-convection flow past an accelerated vertical plate

Mech. Res. Commun., 12 (1985), pp. 31-40

 [View PDF](#) [View article](#) [View in Scopus ↗](#) [Google Scholar ↗](#)

- [15] B. Hemalatha, S. Sathiamoorthy
Effect of cerebrospinal fluid dynamics with hydrocephalus in porous medium
Turkish J. Comput. Math. Educ., 12 (2021), pp. 5666-5671
[Google Scholar ↗](#)
- [16] B. Hemalatha, S. Senthamil Selvi
Effect of suction on an unsteady congenital hydrocephalus in cerebrospinal fluid flow between porous plates with thermal diffusion
Int. J. Res. Educ. Sci. Methods, 9 (2021)
[Google Scholar ↗](#)
- [17] H. Balasundaram, S. Sathiamoorthy, S.S. Santra, *et al.*
Effect of ventricular elasticity due to congenital hydrocephalus
Symmetry, 13 (2021), p. 2087
[CrossRef ↗](#) [View in Scopus ↗](#) [Google Scholar ↗](#)
- [18] S. Gholampour
FSI simulation of CSF hydrodynamic changes in a large population of non-communicating hydrocephalus patients during treatment process with regard to their clinical symptoms
PLoS One, 13 (2018), Article e0196216
[CrossRef ↗](#) [View in Scopus ↗](#) [Google Scholar ↗](#)
- [19] S. Gholampour, N.Fatourae Seifollah, A.S. Seddighi, *et al.*
Evaluating the effect of hydrocephalus cause on the manner of changes in the effective parameters and clinical symptoms of the disease
J. Clin. Neurosci., 35 (2017), pp. 50-55
 [View PDF](#) [View article](#) [View in Scopus ↗](#) [Google Scholar ↗](#)
- [20] S. Gholampour, M. Bahmani
Hydrodynamic comparison of shunt and endoscopic third ventriculostomy in adult hydrocephalus using in vitro models and fluid-structure interaction simulation
Comput. Methods Programs Biomed., 204 (2021), Article 106049
 [View PDF](#) [View article](#) [View in Scopus ↗](#) [Google Scholar ↗](#)
- [21] P. Thiyagarajan, S. Sathiamoorthy, H. Balasundaram, *et al.*
Mass transfer effects on mucus fluid in the presence of chemical reaction
Alexandria Eng. J. (2022)
[Google Scholar ↗](#)
- [22] P. Thiyagarajan, S. Sathiamoorthy, S. Santra, *et al.*

Free and forced convective flow in pleural fluid with effect of injection between different permeable regions

Coatings, 11 (2021), p. 1313

[CrossRef ↗](#) [View in Scopus ↗](#) [Google Scholar ↗](#)

[23] T. Padmavathi, S. Senthamilselvi, S. Santra, *et al.*

Rotational reaction over infected COVID-19 on human respiratory tract in the presence of solet effect with Hall current, The bulletin of Irkutsk State University

Geoarchaeol. Ethnol. Anthropol. Ser., 40 (2022), pp. 15-33

[CrossRef ↗](#) [View in Scopus ↗](#) [Google Scholar ↗](#)

[24] E.A. Vijayalakshmi, S.S. Santra, T. Botmart, *et al.*

Analysis of the magnetohydrodynamic flow in a porous medium

AIMS Math., 7 (2022), pp. 15182-15194

[View in Scopus ↗](#) [Google Scholar ↗](#)

[25] S. Gholampour, N. Fatourae

Boundary conditions investigation to improve computer simulation of cerebrospinal fluid dynamics in hydrocephalus patients

Commun. Biol., 4 (2021), pp. 1-15

[CrossRef ↗](#) [Google Scholar ↗](#)

Cited by (2)

[Galerkin computational work on thermally enhancement process in complex rheological generalized theory due to 3D-partially ionized rotational flow](#)

2023, Case Studies in Thermal Engineering

[Show abstract](#) 

[Performance analysis of annular disks with non-Newtonian Rabinowitsch fluid model: Influence of squeeze film pressure, surface roughness, porosity and viscosity variation ↗](#)

2023, International Journal of Modern Physics B

© 2022 The Author(s). Published by Elsevier Ltd on behalf of The Chinese Society of Theoretical and Applied Mechanics.



All content on this site: Copyright © 2024 Elsevier B.V., its licensors, and contributors. All rights are reserved, including those for text and data mining, AI training, and similar technologies. For all open access content, the Creative Commons licensing terms apply.

